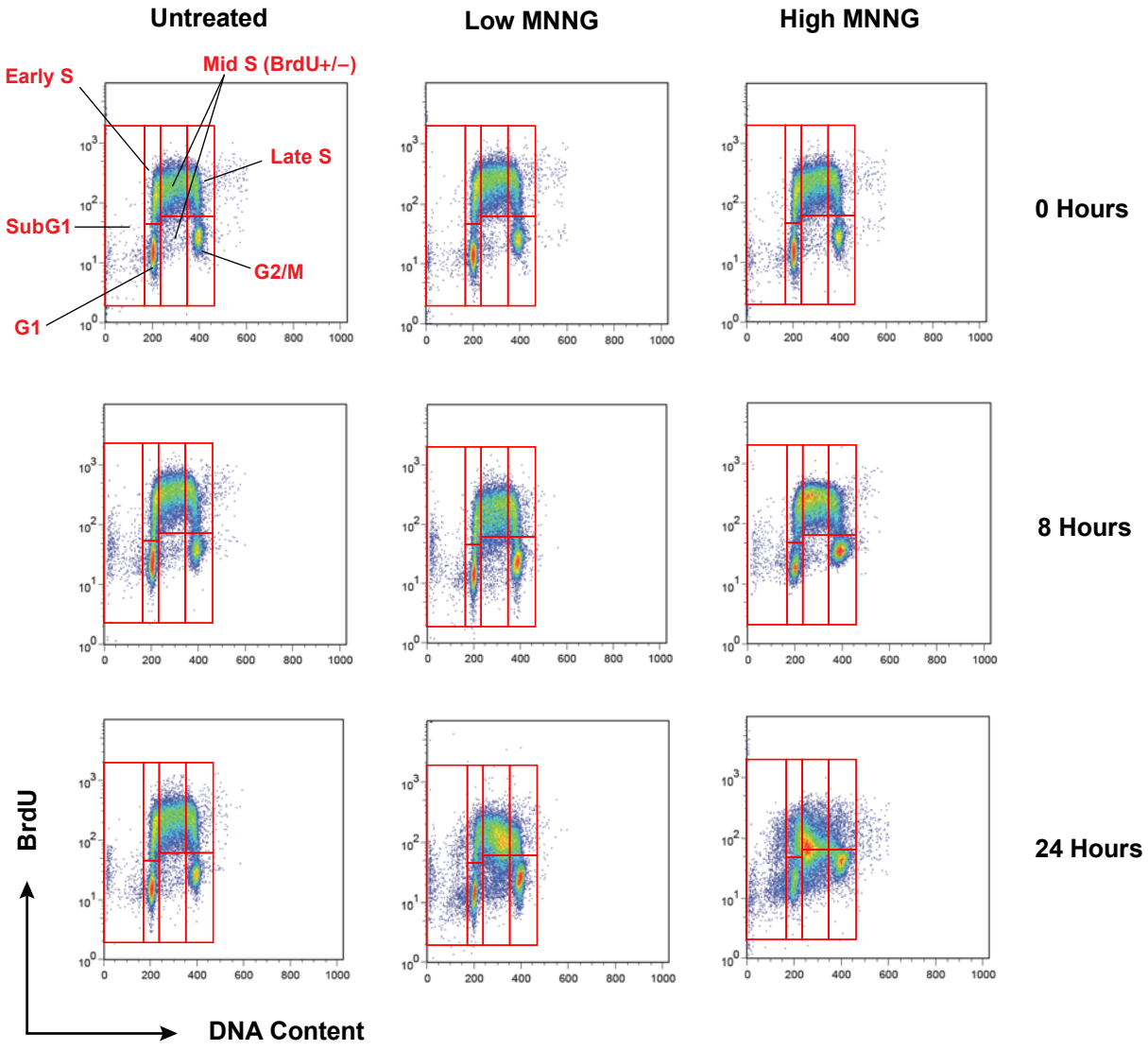

Figure S1. Characterization of cell cycle progression combining measurements of active DNA synthesis and total DNA content.

Representative cell cycle plots for TK6 cells treated with 0 µg/ml (untreated), 0.01 µg/ml (low dose), or 0.1 µg/ml (high dose) MNNG are illustrated. One hour prior to the time point indicated BrdU was added to the culture medium, allowing for its incorporation into actively replicating DNA. Flow cytometry plots of BrdU intensity versus DNA content are shown along with a representation of the gating used to quantitate the amount of cells in each cell cycle stage. G1 and G2/M cells are BrdU negative with 2N and 4N DNA content respectively. Mid S-phase cells have intermediate DNA content and are either BrdU positive or BrdU negative depending on their replication status. The transitions

between these states are labeled early S-phase and late S-phase. Early S-phase cells and late S-phase cells stain positive for BrdU but contain G1 and G2/M DNA content respectively. In addition, apoptotic cells are identified by subG1 DNA content.

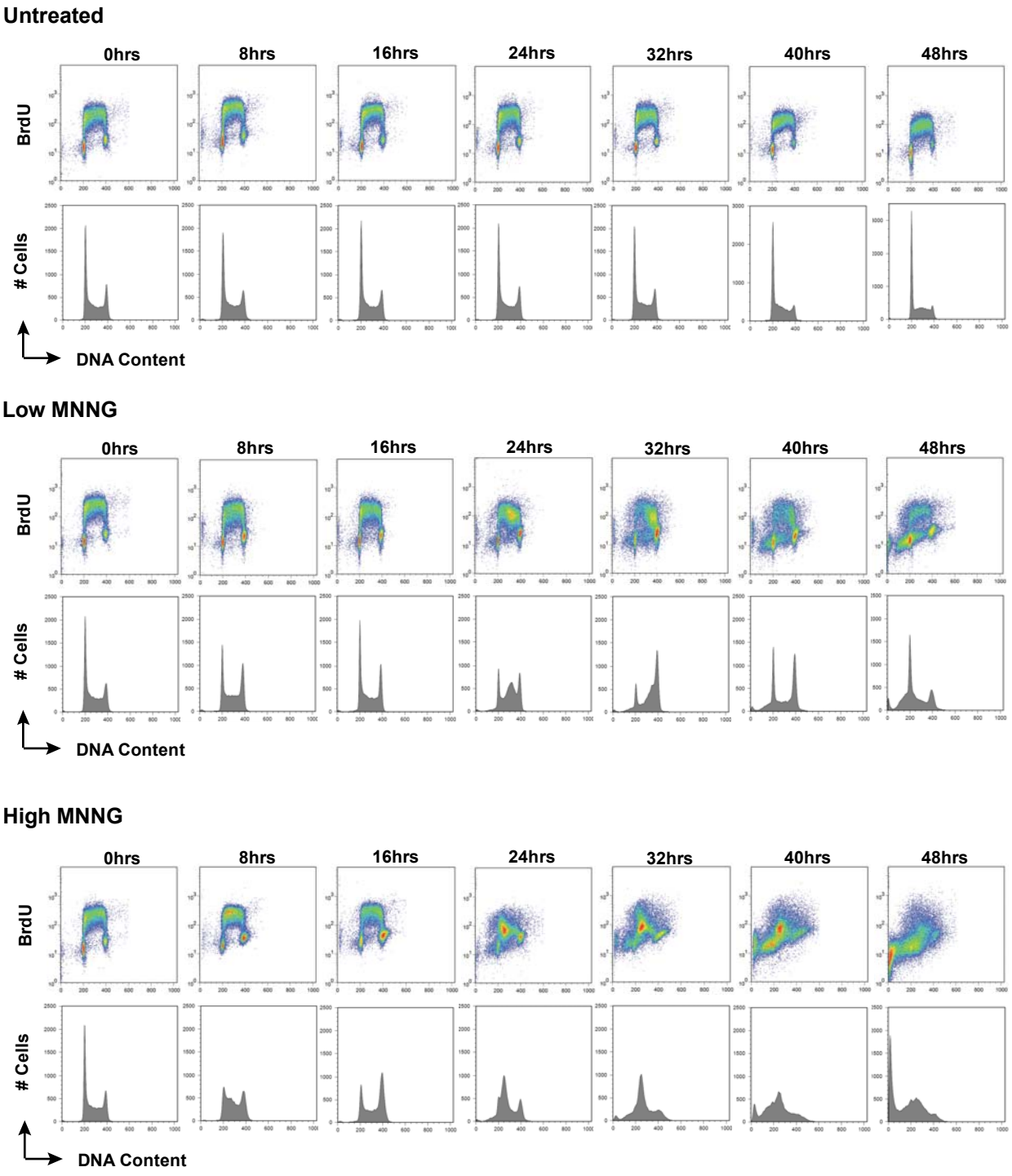

Figure S2. TK6 cell cycle dynamics following MNNG exposure.

TK6 cells were exposed to 0 μg/ml (untreated), 0.01 μg/ml (low dose), or 0.1 μg/ml (high dose) MNNG and the cell cycle was analyzed at the indicated times following treatment. Shown are representative BrdU versus DNA content scatter plots alongside their corresponding DNA content histograms.

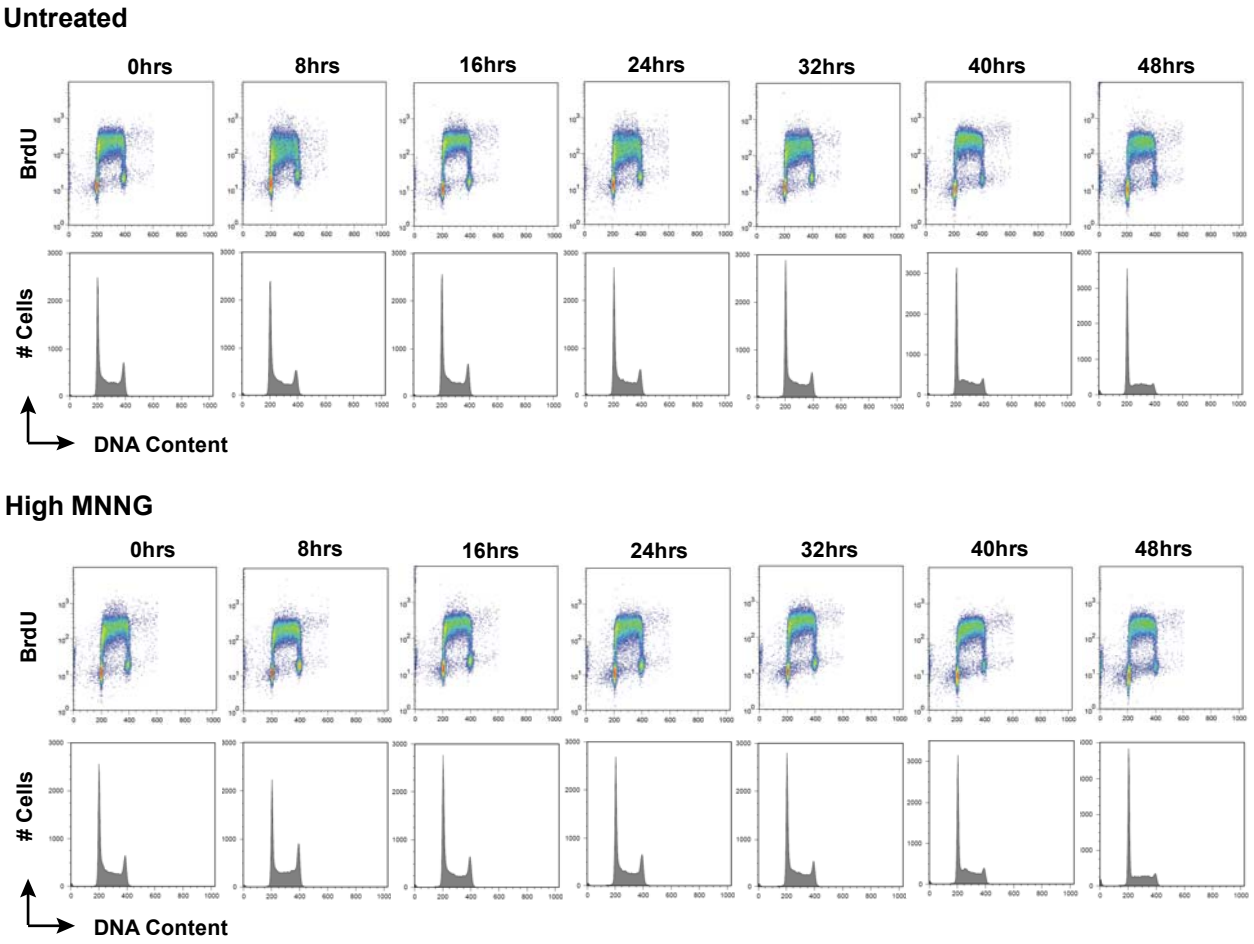

Figure S3. TK6/MGMT$^+$ cell cycle dynamics following MNNG exposure.

TK6/MGMT$^+$ cells were exposed to 0 μg/ml (untreated) or 0.1 μg/ml (high dose) MNNG and the cell cycle was analyzed at the indicated times following treatment. Shown are representative BrdU versus DNA content scatter plots alongside their corresponding DNA content histograms.

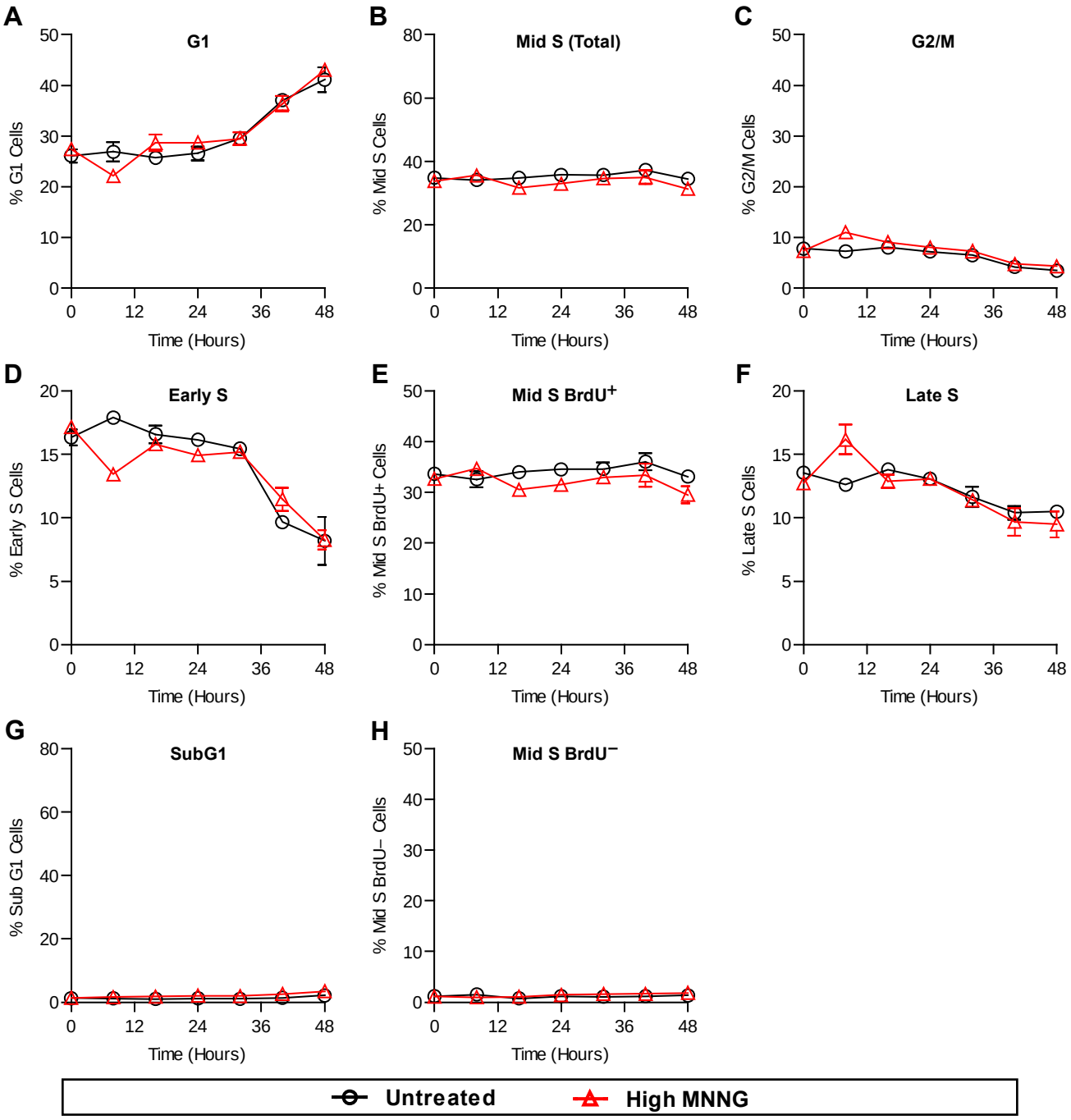

Figure S4. *O*^{6}MeG repair by MGMT eliminates cell cycle perturbations induced by MNNG.

(A-H) Cells were pulse labeled with BrdU for one hour prior to the indicated time point and subsequently analyzed for the incorporation of BrdU into replicating DNA and for total DNA content. Plotted is the percentage of TK6/MGMT$^+$ cells in each phase of the cell cycle following treatment with 0 μg/ml (⊖) or 0.1 μg/ml (△) MNNG. For all panels, the means and standard deviations for two

independent experimental replicates are shown (error bars appear absent when they are smaller than the symbol). Note that the axes are on different scales to highlight the dynamics of each of the cell cycle stages.

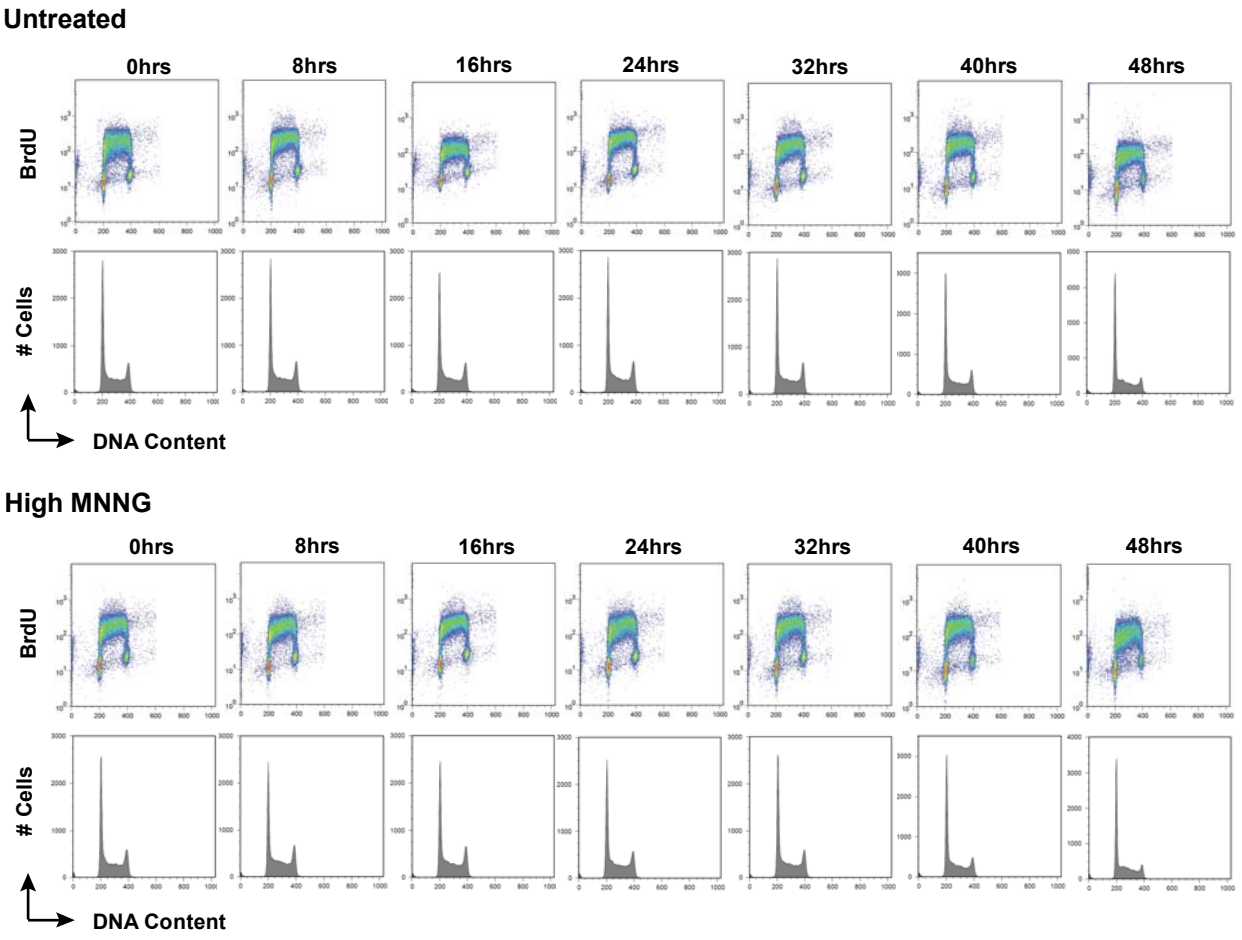

Figure S5. TK6/MMR⁻ cell cycle dynamics following MNNG exposure.

TK6/MMR⁻ cells were exposed to 0 μg/ml (untreated) or 0.1 μg/ml (high dose) MNNG and the cell cycle was analyzed at the indicated times following treatment. Shown are representative BrdU versus DNA content scatter plots alongside their corresponding DNA content histograms.

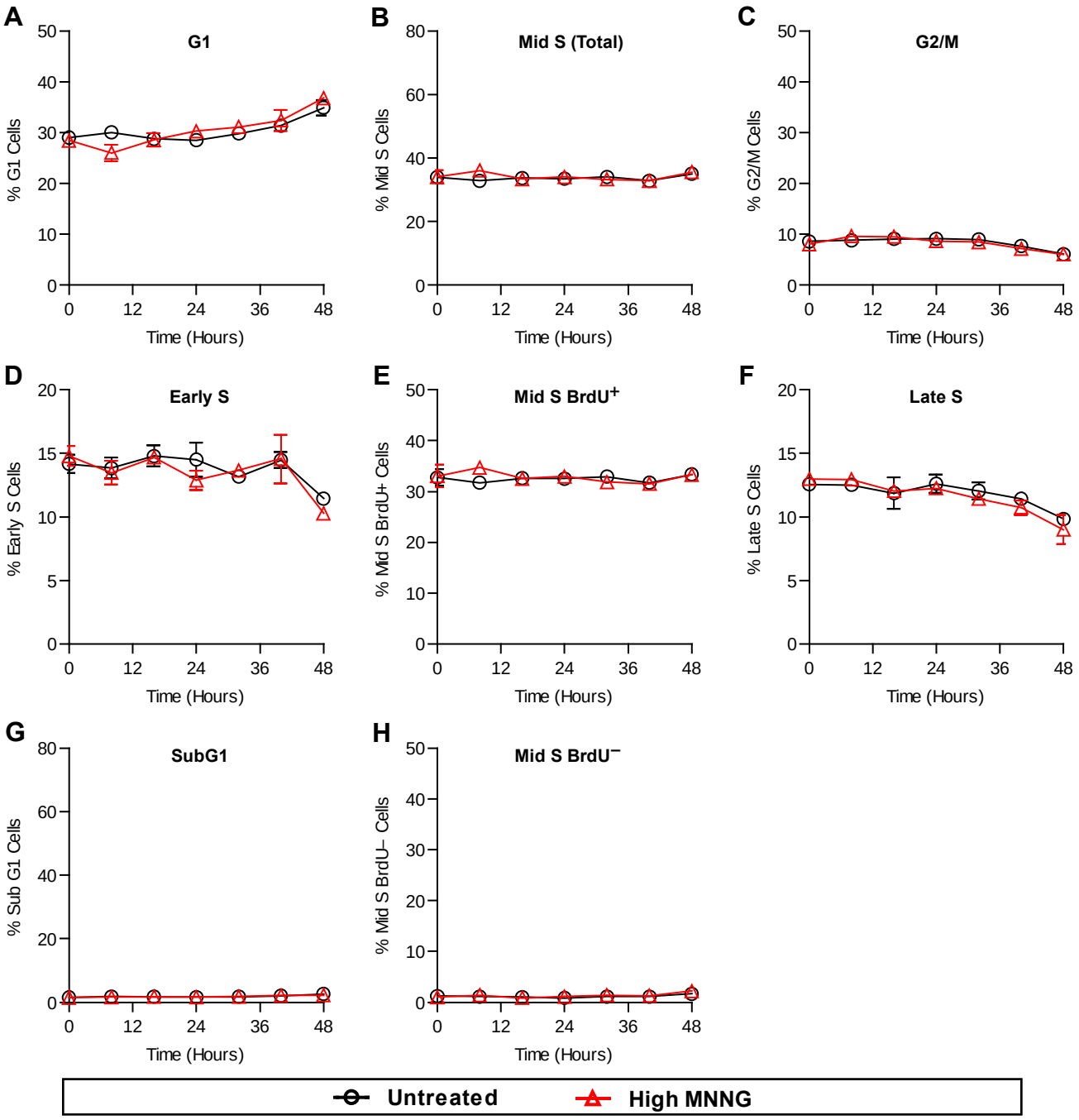

Figure S6. MNNG-induced cell cycle perturbations are MMR dependent.

(A-H) Cells were pulse labeled with BrdU for one hour prior to the indicated time point and subsequently analyzed for the incorporation of BrdU into replicating DNA and for total DNA content. Plotted is the percentage of TK6/MMR$^-$ cells in each phase of the cell cycle following treatment with 0 µg/ml (⊖) or 0.1 µg/ml (△) MNNG. For all panels, the means and standard deviations for two

independent experimental replicates is shown (error bars appear absent when they are smaller than the symbol). Note that the axes are on different scales to highlight the dynamics of each of the cell cycle stages.

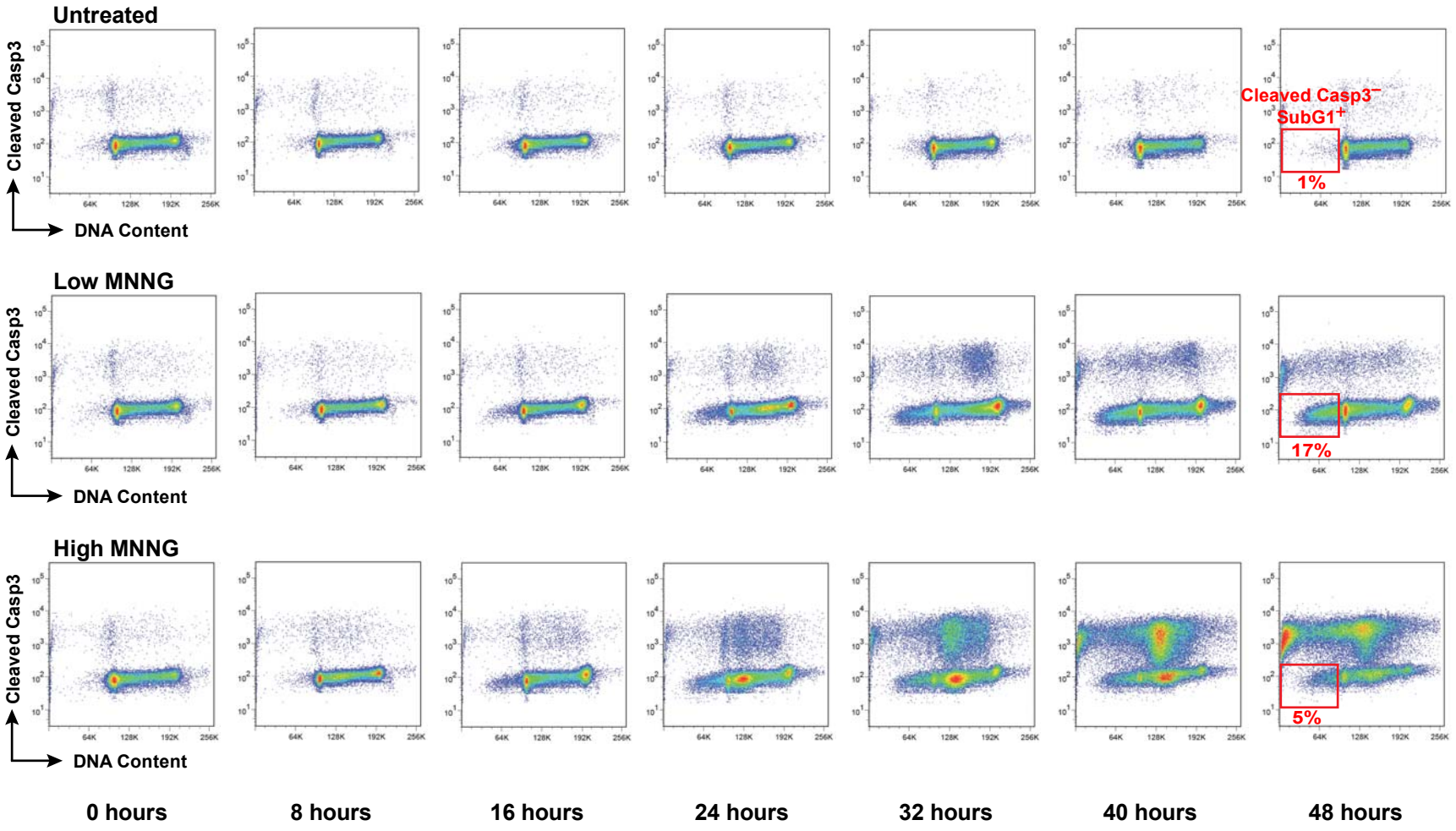

Figure S7. Caspase-3 is activated in S-phase of the second cell cycle following TK6 cell treatment with MNNG.

TK6 cells were treated with 0 μg/ml (untreated), 0.01 μg/ml (low dose), or 0.1 μg/ml (high dose) MNNG and analyzed for cleaved (active) caspase-3 along with DNA content. Shown are representative flow cytometry plots of cleaved caspase-3 versus DNA content over a period of 48 hours post MNNG treatment.

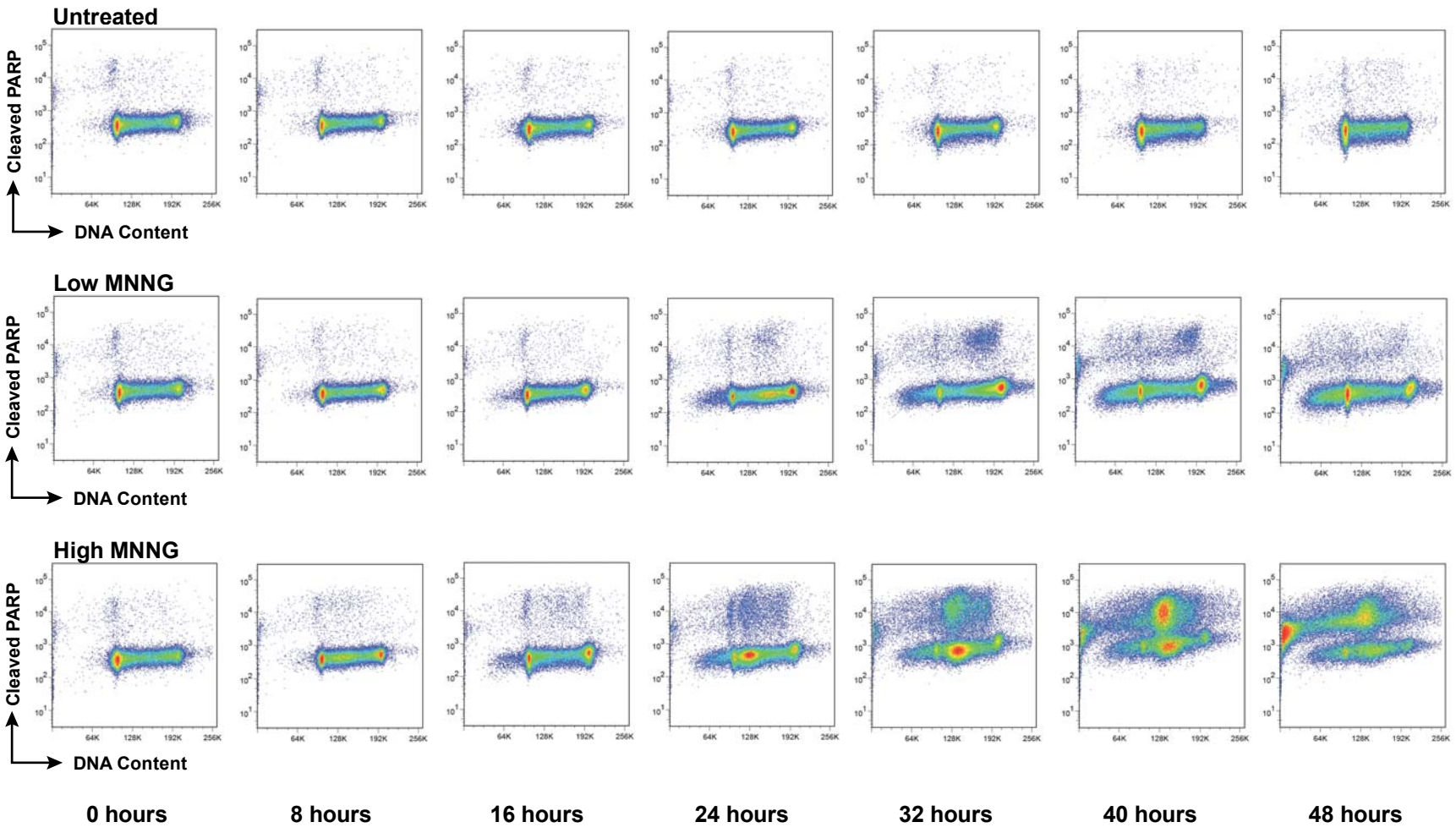

Figure S8. Cleaved PARP is induced in S-phase of the second cell cycle following TK6 cell treatment with MNNG.

TK6 cells were treated with 0 μg/ml (untreated), 0.01 μg/ml (low dose), or 0.1 μg/ml (high dose) MNNG and analyzed for cleaved (inactive) PARP along with DNA content. Shown are representative flow cytometry plots of cleaved PARP versus DNA content over a period of 48 hours post MNNG treatment.

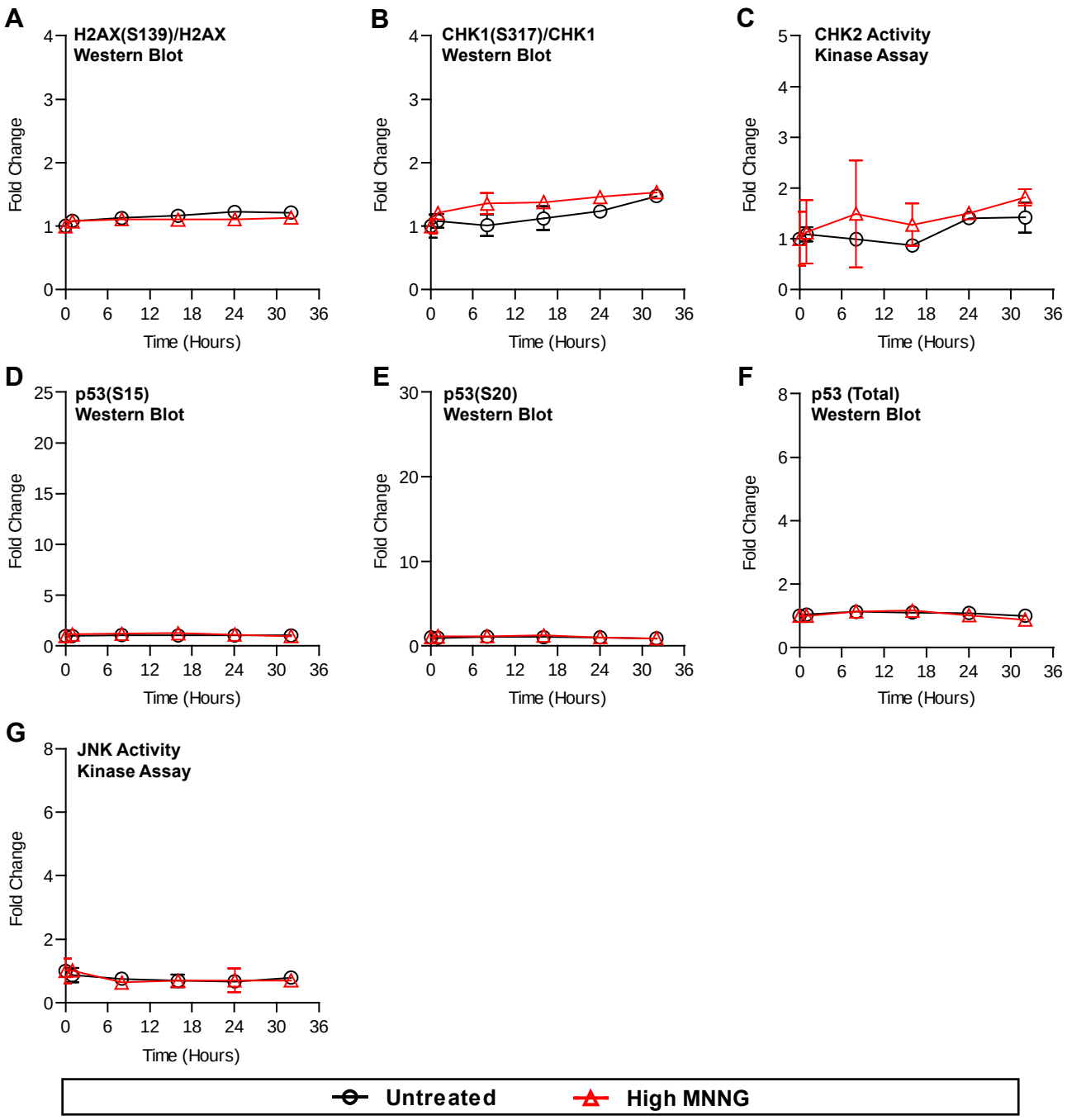

Figure S9. MNNG-induced signaling response is *O*^{6}MeG dependent.

Phosphorylation or activation of DNA damage signaling proteins were monitored by western blot or kinase activity assay, respectively, after TK6/MGMT$^+$ cell treatment with 0 µg/ml (⊖) or 0.1 µg/ml (△) MNNG. All western blot results were normalized to actin as a loading control. For the indicated proteins, phosphorylation levels were additionally normalized to total levels. Phosphorylation and

kinase activity results are plotted as fold change relative to 0 hours. The means and standard deviations for two independent experimental replicates are shown (error bars appear absent when they are smaller than the symbol). Filled symbols represent a significant difference between treated and untreated values at the indicated time point (p-value<0.05, two sample t-test).

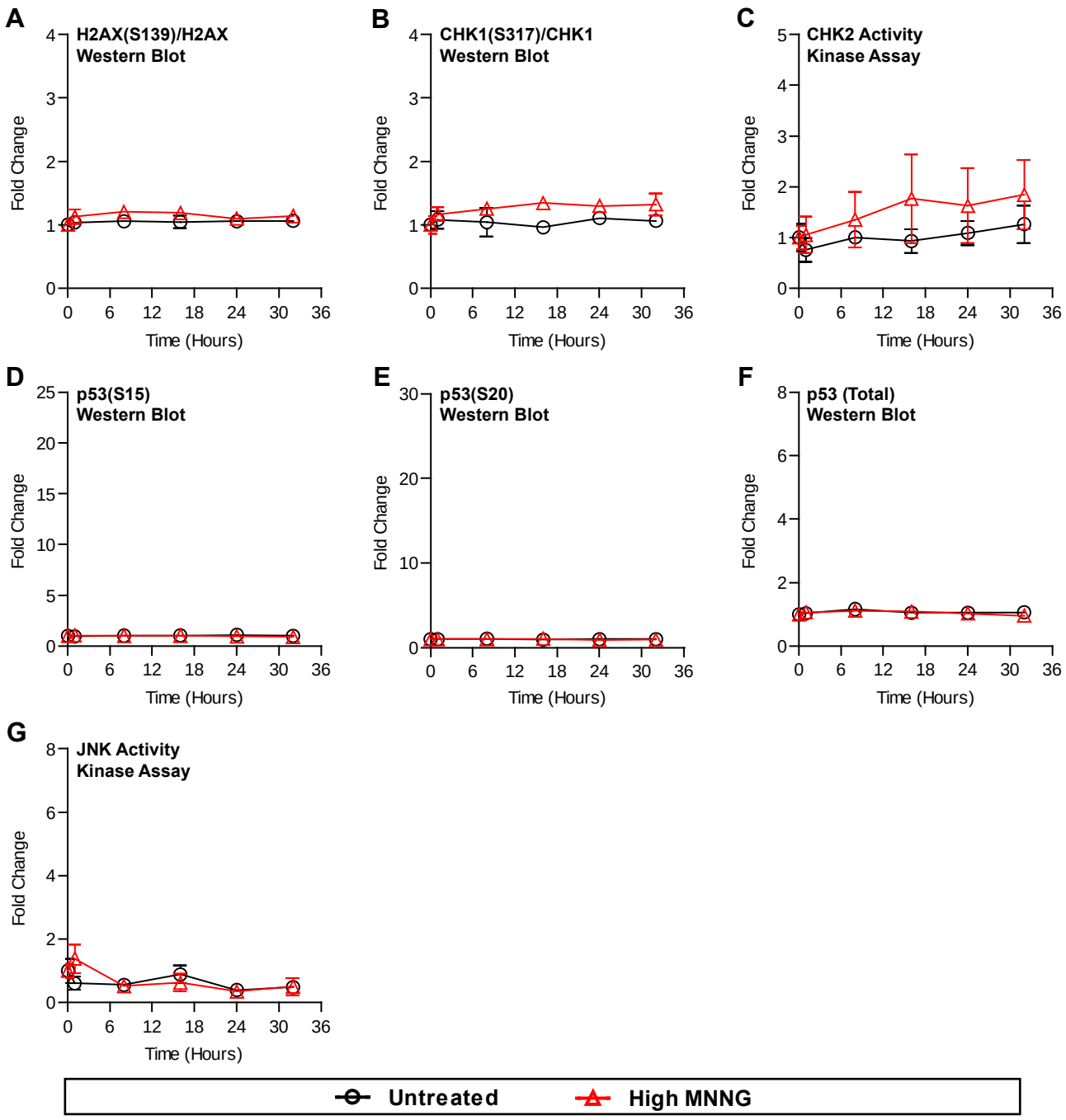

Figure S10. MMR is required for activation of signaling response triggered by O^6MeG.

Phosphorylation or activation of DNA damage signaling proteins were monitored by western blot or kinase activity assay, respectively, after TK6/MMR⁻ cell treatment with 0 µg/ml (⊖) or 0.1 µg/ml (△) MNNG. All western blot results were normalized to actin as a loading control. For the indicated proteins, phosphorylation levels were additionally normalized to their total levels. Phosphorylation and

kinase activity results are plotted as fold change relative to 0 hours. The means and standard deviations for two independent experimental replicates are shown (error bars appear absent when they are smaller than the symbol). Filled symbols represent a significant difference between treated and untreated values at the indicated time point (p-value<0.05, two sample t-test).

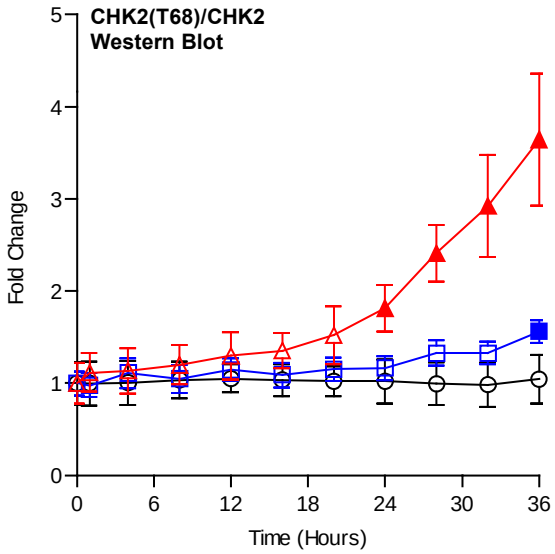

Figure S11. MNNG exposure results in CHK2 phosphorylation.

CHK2 phosphorylation at threonine-68 was monitored in TK6 cells following treatment with 0 µg/ml (⊖), 0.01 µg/ml (⊟), or 0.1 µg/ml (△) MNNG. CHK2(T68) levels were normalized to total CHK2 levels. Results are plotted as fold change relative to 0 hours. The means and standard deviations for three independent experimental replicates are shown (error bars appear absent when they are smaller than the symbol). Filled symbols represent a significant difference between treated and untreated values at the indicated time point (p-value<0.05, two sample t-test).

Table S1. Kinase Activity Assay Experimental Conditions

Kinase	Antibody	Substrate	ATP (μM)	[^{32}P]ATP (μCi)	Reaction Time (min)	Termination
CHK2	Anti-Chk2	MK2tide	25	2	60	EDTA
ERK	Anti-Erk1/2	Myelin basic protein	25	1	60	H_3PO_4
JNK	Anti-JNK1	GST-ATF2 (1-109)	10	2	60	H_3PO_4
MK2	Anti-MAPKAPK2	MK2tide	25	2	60	EDTA

Table S2. Western Blot Experimental Conditions

Protein	Cell Lysate (µg)	Gel	Buffer	Membrane	Antibody	Dilution
ATM(S1981)	30	3-8% Tris-Acetate	TA	Nitrocellulose	R&D Systems AF1655	1:750
ATM	30	3-8% Tris-Acetate	TA	Nitrocellulose	Santa Cruz sc-23921	1:200
H2AX(S139)	25	4-12% Bis-Tris	MOPS	PVDF	Upstate 05-636	1:5000
H2AX	25	4-12% Bis-Tris	MOPS	PVDF	Upstate 07-627	1:5000
CHK1(S317)	25	4-12% Bis-Tris	MOPS	PVDF	Bethyl Laboratories BL229	1:1000
CHK1	25	4-12% Bis-Tris	MOPS	PVDF	Santa Cruz sc-8408	1:400
CHK2(T68)	25	4-12% Bis-Tris	MOPS	Nitrocellulose	Abcam ab3501	1:1000
CHK2	25	4-12% Bis-Tris	MOPS	Nitrocellulose	Santa Cruz sc-8813	1:400
p53(S15)	25	10% Bis-Tris	MOPS	PVDF	R&D Systems AF1043	1:1333
p53(S20)	25	10% Bis-Tris	MOPS	PVDF	R&D Systems AF2286	1:2000
p53	25	10% Bis-Tris	MOPS	PVDF	Santa Cruz sc-263	1:400
Actin					Sigma A5441	1:6250